

Glucose-Containing Diblock Polycations Exhibit Molecular Weight, Charge, and Cell-Type Dependence for pDNA Delivery

Yaoying Wu,[†] Miao Wang,[‡] Dustin Sprouse,[†] Adam E. Smith,[§] and Theresa M. Reineke*,[†]

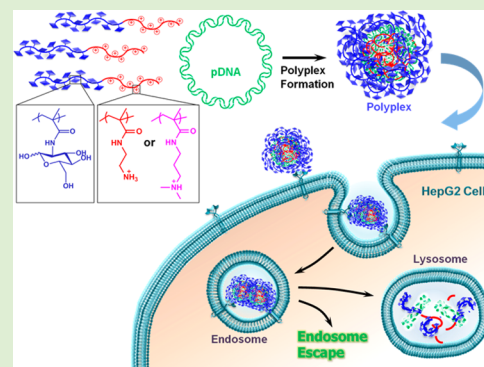
[†]Department of Chemistry, University of Minnesota, 207 Pleasant Street SE, Minneapolis, Minnesota 55455, United States

[‡]Department of Chemical Engineering and Material Science, University of Minnesota, 421 Washington Avenue SE, Minneapolis, Minnesota 55455, United States

[§]Department of Chemical Engineering, University of Mississippi, 134 Anderson, University, Mississippi 38677, United States

Supporting Information

ABSTRACT: A series of diblock glycopolycations were created by polymerizing 2-deoxy-2-methacrylamido glucopyranose (MAG) with either a tertiary amine-containing monomer, *N*-[3-(*N,N*-dimethylamino) propyl] methacrylamide (DMAPMA), or a primary amine-containing unit, *N*-(2-aminoethyl) methacrylamide (AEMA). Seven structures were synthesized via aqueous reversible addition–fragmentation chain transfer (RAFT) polymerization that varied in the block lengths of MAG, DMAPMA, and AEMA along with two homopolymer controls of DMAPMA and AEMA that lacked a MAG block. The polymers were all able to complex plasmid DNA into polyplex structures and to prevent colloidal aggregation of polyplexes in physiological salt conditions. In vitro transfection experiments were performed in both HeLa (human cervix adenocarcinoma) cells and HepG2 (human liver hepatocellular carcinoma) cells to examine the role of charge type, block length, and cell type on transfection efficiency and toxicity. The glycopolymer vehicles with primary amine blocks and PAEMA homopolymers revealed much higher transfection efficiency and lower toxicity when compared to analogs created with DMAPMA. Block length was also shown to influence cellular delivery and toxicity; as the block length of DMAPMA increased in the glycopolymer-based polyplexes, toxicity increased while transfection decreased. While the charge block played a major role in delivery, the MAG block length did not affect these cellular parameters. Lastly, cell type played a major role in efficiency. These glycopolymers revealed higher cellular uptake and transfection efficiency in HepG2 cells than in HeLa cells, while homopolymers (PAEMA and PDMAPMA) lacking the MAG blocks exhibited the opposite trend, signifying that the MAG block could aid in hepatocyte transfection.



INTRODUCTION

Polycations have been extensively studied as macromolecular delivery agents, as they possess the ability to form complexes (i.e., polyplexes) with various polynucleotides such as plasmid DNA (pDNA), small interfering RNA (siRNA), and micro-RNA (miRNA) and to deliver nucleic acids into different cell types.^{1,2} For the purpose of therapeutic development, polyplexes need to provide protection from interaction with plasma proteins, aggregation, and clearance by the reticuloendothelial system (RES) if administered systemically. It becomes apparent that antifouling properties are necessary to achieve successful *in vivo* delivery.^{3,4} Different types of neutral hydrophilic components, such as poly(ethylene glycol) (PEG),^{3–5} zwitterion,^{6–8} and carbohydrates,^{9–15} have been incorporated into polycation delivery systems and studied as stealth coatings. Despite the wide utilization of these stealth agents, such hydrophilic coatings can sterically hinder the interaction between polyplexes and cellular membranes, resulting in lower transfection efficiency.⁴ Additionally, recent studies have found that PEG-containing delivery systems could promote antibody secretion and exhibit clearance from the

bloodstream after repeated injections under certain conditions.^{16,17} These recent findings reinforce the need to design and develop new stealth coatings for drug and gene delivery systems.

Polymeric coatings created from carbohydrates have the ability to improve hydrophilic and steric protective coverage, and may provide the dual benefit of enhancing specific biological interactions through the “glycocluster effect”, which involves binding between multiple carbohydrate molecules along polymer backbones and membrane receptors.^{14,18} Fernandez-Garcia et al. demonstrated that amphiphilic di- and triblock glycopolymers are able to self-assemble into micelles in aqueous media and the obtained micelles could bind with Concanavalin A lectin protein through the “glycocluster effect”.^{19,20} Eun-Ho Song et al. have also designed glycopolymers with mannose and glucose moieties. By taking advantage of the “glycocluster effect”, they established the targeting effect

Received: January 24, 2014

Revised: March 11, 2014

Published: March 13, 2014

of glycopolymers on alveolar macrophages both in vitro and in vivo and studied the activation pathways.²¹ Cationic block glycopolymers with controlled molecular weights have been designed as gene delivery vehicles by our group and others.^{9–13,15,22} Owing to these advantages, glycopolymers received significant research interest for delivery vehicle development.

Controlled architecture, molecular weight, and dispersity are essential for thoroughly examining the impact of polymer structure on transfection efficiency. These properties can be achieved with the help of recent progress in reversible-deactivation radical polymerization (RDRP) techniques, such as nitroxide-mediated polymerization (NMP),²³ atom transfer radical polymerization (ATRP),²⁴ and reversible addition–fragmentation chain transfer polymerization (RAFT).²⁵ Among these controlled polymerization methods, RAFT polymerization has been widely utilized for the synthesis of drug and polynucleotide vehicles because it is suitable for a variety of solvents, reaction conditions, and monomer functional groups.^{22,26} For example, McCormick and co-workers have designed a series of chain transfer agents (CTAs) for aqueous RAFT (co)polymerization.^{27–29} They successfully synthesized a series of cationic copolymers with *N*-2-hydroxypropyl methacrylamide (HPMA) and *N*-[3-(*N,N*-dimethylamino)-propyl]methacrylamide (DMAPMA) for siRNA delivery via aqueous RAFT polymerization, conjugated with folic acid as a targeting moiety. The obtained cationic polymers were evaluated for the ability to deliver siRNA and down regulate the mRNA in cells via the quantitative real-time reverse transcription polymerase chain reaction (qRT-PCR).^{30–32}

In this study, we report our efforts to synthesize and study a family of block coglycopolycations consisting of a hydrophilic block, 2-deoxy-2-methacrylamido glucopyranose (MAG), copolymerized with either DMAPMA or *N*-(2-aminoethyl)-methacrylamide (AEMA) for pDNA complexation and delivery. Previously, our group showed that PMAG-*b*-PAEMAs were able to form polyplexes with pDNA and siRNA, and shield polyplexes from aggregation in physiological salt and serum conditions.⁹ The colloidal stability of the polyplexes was attributed to the incorporation of a PMAG block, which is exposed on the surface of the nanocomplexes, which contain a core structure of the polycation block bound to the nucleic acid. Such “core–shell” structures in aqueous salt and serum solutions have been shown to promote steric shielding of polyplexes to prevent aggregation in biological conditions.^{9,10,33,34} Herein, seven diblock glycopolymers have been synthesized along with two cationic homopolymer controls lacking a poly(MAG) block, PAEMA and PDMAPMA, to examine the effect of the PMAG and charge block lengths and charge type in pDNA binding and delivery in two cultured cell types both HeLa (human cervix adenocarcinoma) cells and HepG2 (human liver hepatocellular carcinoma) cells. The current report also concentrates on understanding and comparing the properties between incorporating a primary amine PAEMA block and a tertiary amine PDMAPMA block, along with block length on the complex formation and delivery of nucleic acids.

EXPERIMENTAL SECTION

Materials. All chemicals were purchased from Sigma Aldrich and used without further purification unless specified otherwise. *N*-(2-aminoethyl) methacrylamide hydrochloride (AEMA·HCl) and *N*-[3-(*N,N*-dimethylamino)propyl]methacrylamide (DMAPMA) were pur-

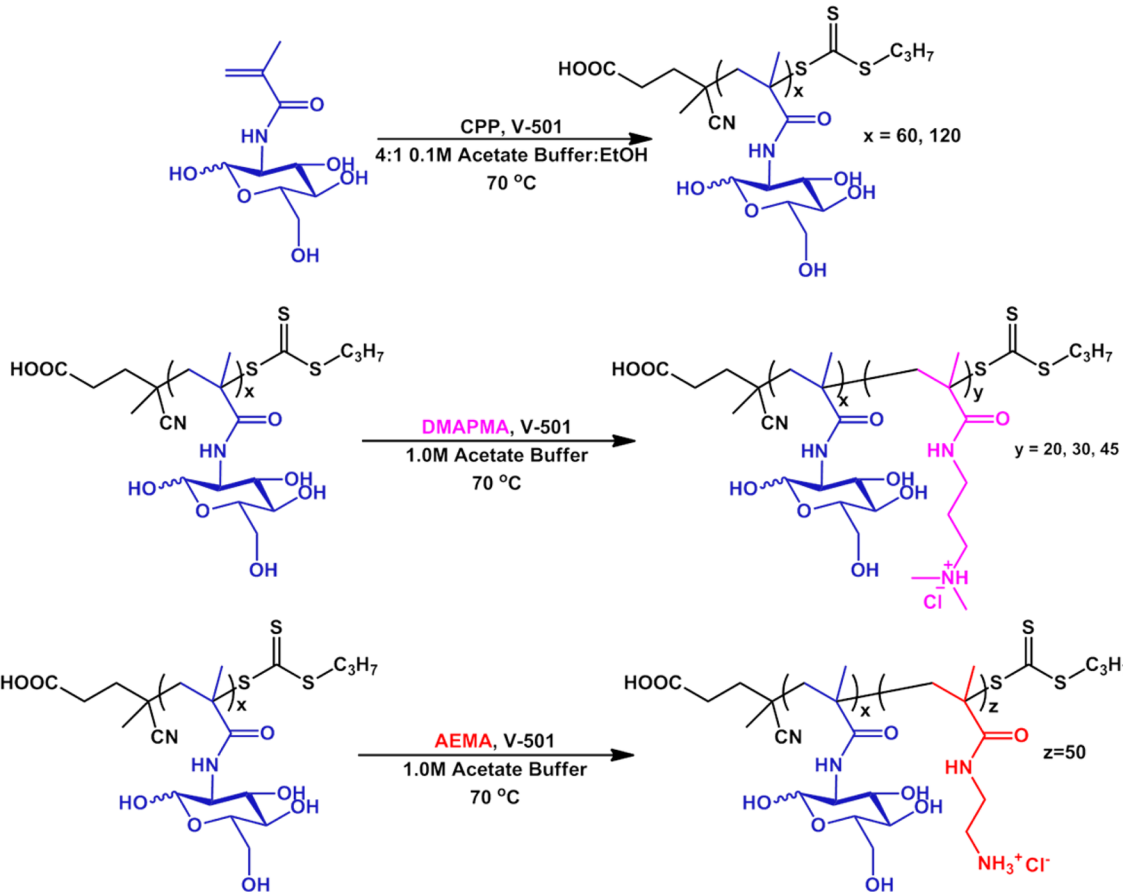
chased from Polyscience, Inc. (Warrington, PA), and DMAPMA was purified via vacuum distillation prior to use. 4,4'-Azobis(4-cyanovaleric acid) (V-501) was recrystallized from methanol. 2-deoxy-2-methacrylamido glucopyranose (MAG)³⁵ and the chain transfer agent (CTA) 4-cyano-4-(propylsulfanylthiocarbonyl) sulfanylpentanoic acid (CPP)²⁹ were synthesized according to previous reports. Cell culture media, Dulbecco's Modified Eagle Medium (DMEM) and Opti-MEM, antibiotic/antimycotic, fetal bovine serum (FBS), phosphate-buffered saline (PBS), and nuclease-free water were purchased from Gibco (Carlsbad, CA). HeLa (Human cervix adenocarcinoma) cells and HepG2 (human liver hepatocellular carcinoma) cells were purchased from ATCC (Rockville, MD). JetPEI was purchased from Polyplus-Transfection Inc. (Illkirch, France). Glycofect was provided by Techlon (Blacksburg, VA) as a gift. 3-[4,5-Dimethylthiazol-2-yl]2,5-diphenyltetrazolium bromide (MTT) was purchased from Molecular Probes (Eugene, Oregon). Luciferase assay kits were purchased from Promega Corp. (Fitchburg, WI). Protein assay kits were purchased from Bio-Rad Laboratories (Hercules, CA).

Methods. Polymer Synthesis. The diblock glycopolymers were synthesized according to similar methods previously published.⁹ Typically, to yield PMAG as the macromolecular chain transfer agent (macroCTA), MAG (0.23 g, 0.93 mmol), CPP (1.7 mg, 6.2×10^{-3} mmol), and V-501 (0.17 mg, 6.2×10^{-4} mmol) were dissolved in 2.0 mL of a 4:1 mixture of 0.1 M acetate buffer (pH 5.2) and ethanol. The solution was added to a 5 mL round-bottom flask equipped with magnetic stir bar and purged with nitrogen for 50 min before the flask was sealed and placed into a preheated oil bath at 70 °C. The reaction was then terminated by exposure to air at predetermined time points to yield different lengths of PMAG. The two PMAG macroCTAs were purified by dialysis with 3500 Da molecular weight cutoff dialysis tubing against ultrapure water and lyophilized to dryness. To synthesize the diblock glycopolymers, the macroCTA (100 mg, 3.4×10^{-3} mmol for PMAG_{11s}; 52 mg, 3.3×10^{-3} mmol for PMAG₆₁), AEMA·HCl (33 mg, 0.20 mmol) or DMAPMA (34 mg, 0.20 mmol), and V-501 (0.21 mg, 7.5×10^{-4} mmol) were dissolved in 1.2 mL of 1.0 M acetate buffer (pH 5.2) in a 5 mL round-bottom flask. After the solution was purged with nitrogen for 50 min, the polymerization was carried out in a preheated oil bath at 70 °C. Polymerization was terminated at a predetermined time point to yield different molecular weights by exposing the reaction mixture to air. The final product was purified via extensive dialysis with a 3500 Da molecular weight cutoff membrane against water (pH 5–6, pH adjusted by concd HCl) and lyophilization.

To synthesize homopolymers, the CPP (3.0 mg, 1.1×10^{-2} mmol), AEMA·HCl (108.3 mg, 0.66 mmol) or DMAPMA (112.2 mg, 0.66 mmol), and V-501 (0.61 mg, 2.2×10^{-3} mmol) were dissolved in 3.29 mL of a 4:1 mixture of 1.0 M acetate buffer (pH 5.2)/ethanol in a 5 mL round-bottom flask. After the solution was purged with nitrogen for 50 min, the polymerization was carried out in a preheated oil bath at 70 °C for 3 h before termination by exposing the reaction mixture to air. The final product was purified by dialysis with a 3500 Da molecular weight cutoff membrane against water (pH 5–6, adjusted with concd HCl), as described above, and white powder was acquired after lyophilization.

Polymer Characterization. The number average molecular weight (M_n) and dispersity (M_w/M_n) for each polycation was determined by size exclusion chromatography (SEC) equipped with Eprogen columns [CATSEC1000 (7 μm, 50 × 4.6), CATSEC100 (5 μm, 250 × 4.6), CATSEC300 (5 μm, 250 × 4.6), and CATSEC1000 (7 μm, 250 × 4.6)], a Wyatt HELEOS II light scattering detector ($\lambda = 662$ nm), and an Optilab rEX refractometer ($\lambda = 658$ nm). The columns were maintained at 30 °C. An aqueous eluent (0.1 M Na₂SO₄/1 v/v % acetic acid) was utilized at a flow rate of 0.4 mL/min. The $d\eta/dc$ values for each of the polymers were determined offline with the Optilab rEX refractometer.

¹H NMR measurements were performed with a Varian Inova 300 at 70 °C. Samples were dissolved in D₂O (DOD used as the internal standard), and the block copolymer compositions were determined by calculating the ratio between the integrals of resonances of the PMAG block and those of the PAEMA or PDMAPMA block.

Scheme 1. RAFT Polymerization of PMAG_x-*b*-PDMAPMA_y and PMAG_x-*b*-PAEMA_z

Polyplex Formation and Gel Electrophoresis Assay. The ability of each polymer to bind with pDNA and form polyplexes was qualitatively determined by gel electrophoresis. pCMV-luc plasmid DNA (1.0 μ g, 0.02 μ g/ μ L) was mixed with an equal volume of each aqueous polycation solution (which were diluted to form polyplexes at various N/P ratios). The N/P ratio denotes the molar ratio of primary amine or tertiary amine (N) moieties in the amine block to the phosphate (P) groups on the pDNA backbone. After an incubation of 1 h, a 10 μ L aliquot was run in a 0.6% agarose gel containing 6 μ g of ethidium bromide/100 mL TAE buffer (40 mM Tris-acetate, 1 mM ethylenediaminetetraacetic acid (EDTA)) for 45 min at 90 V.

Dynamic Light Scattering (DLS) and ζ Potential. Polyplex sizes were measured by dynamic light scattering (DLS) at 633 nm with a Malvern Zetasizer Nano ZS. pCMV-luc (1.0 μ g, 0.02 μ g/ μ L) was incubated with an equal volume of each polymer at an N/P ratio of 5 and 10 for 1 h to form the subsequent polyplexes. Thereafter, samples were diluted to 300 μ L with either H₂O or Opti-MEM. The samples were measured in triplicate at 25 °C with a detection angle of 173°. For the study of colloidal stability of the polyplexes in Opti-MEM, samples were measured in triplicate at time intervals of 0, 2, and 4 h after dilution with Opti-MEM.

The ζ potential for each polyplex formulation was measured with the same instrument using a detection angle of 17°. The polyplexes were formed in nuclease-free water according to the aforementioned procedure at an N/P ratio of 5 and 10. After a 1 h incubation time, the polyplex solutions were diluted to 900 μ L with nuclease-free water for measurement, and the ζ potential was measured in triplicate.

Cryogenic Transmission Microscopy (CryoTEM). Polyplex solutions were prepared as described above at an N/P ratio of 5. CryoTEM samples were prepared using Vitrobot Mark IV (FEI). A total of 3.0 μ L of polyplex solution was applied onto a lacey Formvar/carbon grid (Ted Pella, Inc.), which was held by a pair of tweezers in humidity controlled (95%) chamber at 22 °C. After the excess solution

was blotted away using filter paper, the grid was quickly plunged into liquid ethane. The vitrified samples were then quickly transferred into liquid nitrogen for storage. For imaging, sample grids were transferred onto a Gatan 626 cryogenic sample holder in liquid nitrogen and examined in FEI Tecnai G² Spirit BioTWIN LaB₆ transmission electron microscope at -178 °C, using an accelerating voltage of 120 kV. Images were recorded using Eagle 2k CCD camera, and analyzed with FEI TEM Imaging and Analysis (TIA) software. Phase contrast was enhanced by imaging at about 10 μ m under focus.

Cell Culture Experiments. Both HeLa cells and HepG2 cells were cultured in high glucose DMEM media with 10% FBS and 1% antibiotic and antimicrobial in a humidified atmosphere containing 5% CO₂ at 37 °C, according to the established protocol (ATCC, Rockville, MD).

Cellular Uptake. Cells were seeded in six-well plates at 250000 cells/well and incubated for 24 h, as described above. Plasmid DNA was labeled with cyanine (Cy5) using a Label-IT Cy5 DNA labeling kit (Mirus, Madison, WI) according to the manufacturer's protocol. Following the procedure previously described above, 500 μ L of polyplexes were prepared by combining Cy5-labeled pDNA and each of the polymer samples at an N/P ratio of 5 and 10. JetPEI and Glycofect were both used to prepare polyplexes at N/P ratios of 5 and 20, respectively, as positive controls. A total of 500 μ L of polyplex solution was diluted with 1.0 mL of Opti-MEM immediately prior to transfection. Each well of cells was treated with 500 μ L of the diluted polyplex solution, followed by a 4 h incubation at 37 °C. Subsequently, the cells were incubated with CellScrub for 5 min after the removal of cell media (to remove surface-bound polyplexes), followed by trypsinization, centrifugation, and then suspension in PBS. BD FACSVersa flow cytometer (San Jose, CA) equipped with a helium-neon laser to excite Cy5 (633 nm) and BD FACSuite software were used for flow cytometry analysis. A total of 10000 events were collected for each sample well. The positive fluorescence level

was established by inspection of the histogram of negative control cells such that <1% appeared in the positive region.

Luciferase Reporter Gene Transfection and Cell Viability. HepG2 or HeLa cells were seeded in 24-well plates at 50000 cells/well and incubated in supplemented DMEM at 37 °C and 5% CO₂ for 24 h. Prior to transfection, 150 μL of Gwiz-luc pDNA (0.02 μg/μL) was combined with 150 μL of each polymer solution at an N/P ratio of 5 and 10 to form polyplexes. As positive controls, the same volume of polyplexes formed with JetPEI (N/P = 5) and Glycofect (N/P = 20) were prepared. After mixing with 600 μL of Opti-MEM, the polyplex solution was added onto the cells. Each well of cells were treated with 300 μL of mixed solution, followed by the addition of 800 μL of supplemented DMEM after 4 h incubation. The cell media was then replaced with 1 mL supplemented DMEM 24 h after transfection. The luciferase or MTT assays were carried out 48 h after transfection. For the luciferase assay, each well of cells were washed with PBS and then treated with 100 μL of lysis buffer (Promega, Madison, WI). A 5 μL aliquot of each well of cell lysate was examined on 96-well plates for luciferase activity with a Synergy H1 Hybrid Reader (BioTek, Winooski, VT). The amount of protein in the cell lysates per sample was determined against a standard curve of bovine serum albumin according to the established protocol from Bio-Rad (Hercules, CA) DC protein assay kit.

For the MTT assay, 48 h after transfection, each well of cells were washed with 0.5 mL PBS and then incubated with 1 mL of supplemented DMEM containing 0.5 mg/mL of 3-[4,5-dimethylthiazol-2-yl]2,5-diphenyltetrazolium bromide (MTT) for 1 h at 37 °C. Following the removal of the DMEM solution containing MTT, the cells were then washed with PBS, and 600 μL of DMSO was added to each well. The 24-well plates were then placed on a shaker for 20 min for dissolution of the purple formazan. Subsequently, a 200 μL aliquot from each well was added into a 96-well plate and analyzed for absorbance intensity at 570 nm.

Asialoglycoprotein (ASGP) Receptor Inhibition Experiment. The experimental procedure was adapted from a previous publication.³⁶ Cells were seeded in 24-well plates at 50000 cells/well in a similar fashion to the previous procedure and incubated at 37 °C for 24 h. Polyplex solutions were prepared at an N/P ratio of 5 using the aforementioned procedure for transgene expression and diluted with Opti-MEM prior to transfection. Prior to cellular exposure to the polyplex solutions, each well of cells was treated with either 200 μL of DMEM containing 0.02 μg/μL galactose or 200 μL of DMEM for 20 min. Subsequently, the cells were treated with 300 μL of polyplex Opti-MEM solution after the removal of the galactose DMEM solution and then incubated at 37 °C for 4 h before 800 μL of supplemented DMEM was added into each well. The cell media was replaced with 1 mL supplemented DMEM 24 h after transfection. A luciferase assay was carried out 48 h after transfection using the same procedure described above.

Statistical Analysis. All data are presented as the mean ± the standard deviation and each analysis or measurement was performed in triplicate unless otherwise noted. For statistical analysis of the data, the means were compared using a Student's *t* test with *p* < 0.05 being considered as statistically significant.

RESULTS AND DISCUSSION

Synthesis and Characterization of Diblock Glycopolymers. Previously, our group reported a series of cationic diblock glycopolymers with various chain lengths and charge species as polymeric gene delivery vehicles.^{9,10} The polyplexes formed from this series of diblock glycopolymers exhibited colloidal stability in cell media and had relatively low cytotoxicity. Moreover, both amine type and cationic charge block length were demonstrated to greatly affect transgene expression efficiency in vitro.¹⁰ To further understand how polymer structure impacts transgene expression, in particular, the role of the sugar and tertiary amine block length, aqueous RAFT polymerization was employed to synthesize well-defined

cationic polymers and their activity was assessed for plasmid DNA delivery. Seven diblock copolymers were synthesized according to Scheme 1. First, the glucose-derived block was synthesized from MAG via RAFT polymerization. Based on the polymerization kinetics determined by ¹H NMR (Supporting Information, Figure S1), two different lengths of PMAG were obtained (DP = 61 and 118) by quenching the polymerization at predetermined time points and characterized by SEC (Supporting Information, Figure S2). Both PMAG derivatives were utilized as a macroCTA for chain extension with either DMAPMA or AEMA to yield the cationic diblock glycopolymers. To prevent the aminolysis of the trithiocarbonate chain end, 1.0 M acetate buffer (pH = 5.2) was selected as the reaction solvent. Various block lengths of DMAPMA were acquired by stopping the polymerization at predetermined time points according to the monomer conversion rate (Supporting Information, Figure S3). For comparison, AEMA derivatives were synthesized with a block length similar to the longest DMAPMA block length. The molecular weight and dispersity of all obtained diblock copolymers were determined by SEC chromatography (Supporting Information, Figure S4). Narrow dispersity ($M_w/M_n \leq 1.1$) of the obtained copolymers indicates a highly controlled polymerization. The composition of the blocks was also confirmed by ¹H NMR (Supporting Information, Figure S5). Additionally, to probe the importance of the glucose block for our glycopolplex delivery system, homopolymers of DMAPMA and AEMA were synthesized as controls for the subsequent studies discussed below (Supporting Information, Scheme S1, Figure S6). The molecular weight and dispersity of all the polymers are summarized in Table 1.

The pDNA binding ability of the obtained copolymers was examined through gel electrophoresis shift assays at various ratios between 0 and 50 (Supporting Information, Figure S7). As shown in the gel images, pDNA migration in the gel was

Table 1. Molecular Weight, Dispersity, and Calculated Degree of Polymerization (DP) of the Polymers Examined in This Study

samples	M_n^a (kDa)	$M_w/M_n^a,c$	MAG DP ^{a,b}	amine DP ^{a,b}
PDMAPMA ₆₀	11.4	1.41		60
PAEMA ₅₈	7.3	1.10		58
PMAG ₆₁	15.6	1.01	61	
PMAG _{61-b-} PDMAPMA ₂₁	19.2	1.02	61	21
PMAG _{61-b-} PDMAPMA ₃₉	22.1	1.10	61	39
PMAG _{61-b-PAEMA₅₃}	24.4	1.01	61	53
PMAG ₁₁₈	29.5	1.03	118	
PMAG _{118-b-} PDMAPMA ₂₂	33.2	1.02	118	22
PMAG _{118-b-} PDMAPMA ₃₀	34.6	1.01	118	30
PMAG _{118-b-} PDMAPMA ₄₃	36.9	1.02	118	43
PMAG _{118-b-PAEMA₅₈}	39.0	1.01	118	58

^aAs determined by aqueous SEC using a flow rate of mL/min of 0.1 M Na₂SO₄ in 1.0 v% acidic acid, Eprogen CATSEC100, CATSEC300, and CATSEC1000 columns, a Wyatt HELEOS II light scattering detector ($\lambda = 662$ nm), and an Optilab rEX refractometer ($\lambda = 658$ nm). ^bAs confirmed by ¹H NMR spectroscopy. ^cNote: the dispersity was lower than the theoretical value for some samples, possibly due to the dialysis purification method.

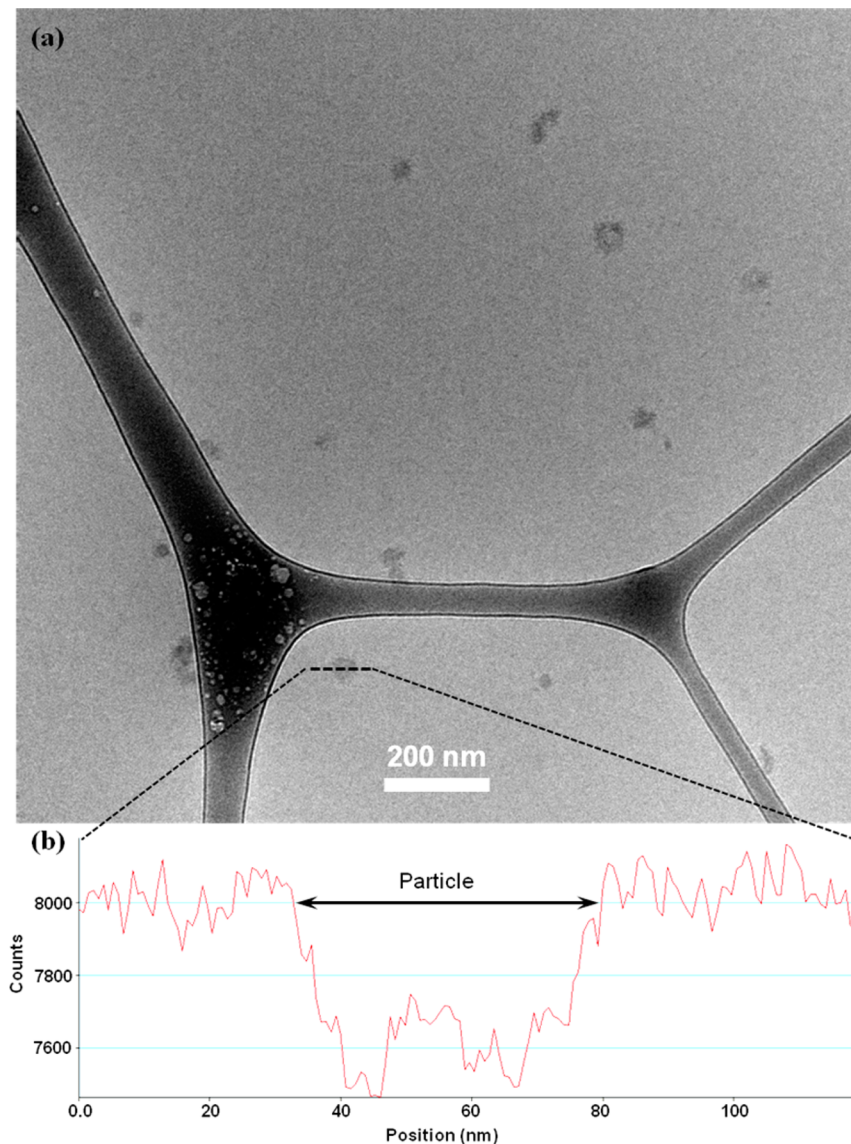


Figure 1. (a) CryoTEM image of a polyplex formed between PMAG₆₁-*b*-PDMapMA₂₁ and pDNA at an N/P ratio of 5; (b) Line profile of counts of electrons vs distance of the polyplex particle highlighted in (a) denoting a diameter of about 45 nm for the polyplex.

completed hindered at N/P ratios above 4 for all of the samples. Therefore, polyplexes formed at N/P ratios of 5 and 10 were selected for further study. The hydrodynamic radius of polyplexes in nuclease-free water was determined to be between 50 and 100 nm via DLS, within the size range for cellular endocytosis (Supporting Information, Figure S8).³⁷ Cryogenic transmission electron microscopy (cryoTEM) was also employed to characterize the native morphology of polyplexes in water. As shown in the representative cryoTEM image (Figure 1), polyplexes in pure water appeared have a circular or "spherical" morphology with some irregularities. Levine et al. reported similar polyplex morphologies formed from branched polyethyleneimine (bPEI) in water via cryoTEM.³⁸ The radii of the particles of all samples were determined via FEI TEM Imaging and Analysis (TIA) software. The radius of polyplexes revealed by cryoTEM was 26 ± 8 nm, slightly lower than the value measured by DLS. It was conceived that the glycopolymers could promote a "core-shell" structure in aqueous solution,^{33,34} where the shell structure might not possess high enough electron density to yield full contrast from that of the

amorphous ice layer. This could cause the discrepancy in size revealed by the cryoTEM data from that revealed via DLS. Zeta potential values of the polyplex solutions formulated at N/P ratios of 5 and 10 in nuclease-free water were all between 10 and 40 mV (Supporting Information, Figure S8). The positive ζ potentials can enhance nonspecific interaction of polyplexes with the cell membrane to trigger cellular uptake.³⁹ The zeta potentials of these polyplexes were also measured in Opti-MEM culture medium (Supporting Information, Figure S9). The values were found to be relatively less positive, ranging from 0 to 10 mV, due to the presence of salt and amino acids in culture medium.

To evaluate the colloidal stability of polyplexes in Opti-MEM (contains physiological salt and small molecule nutrients), the sizes of polyplexes were monitored via DLS over the period of 4 h (Figure 2). As a comparison, the sizes of polyplexes in nuclease-free water were also measured and reported in the graph. Over the experimental period, the polyplexes formed from JetPEI (N/P ratio = 5) and Glycofekt (N/P ratio = 20) aggregated in Opti-MEM with the radius increasing from

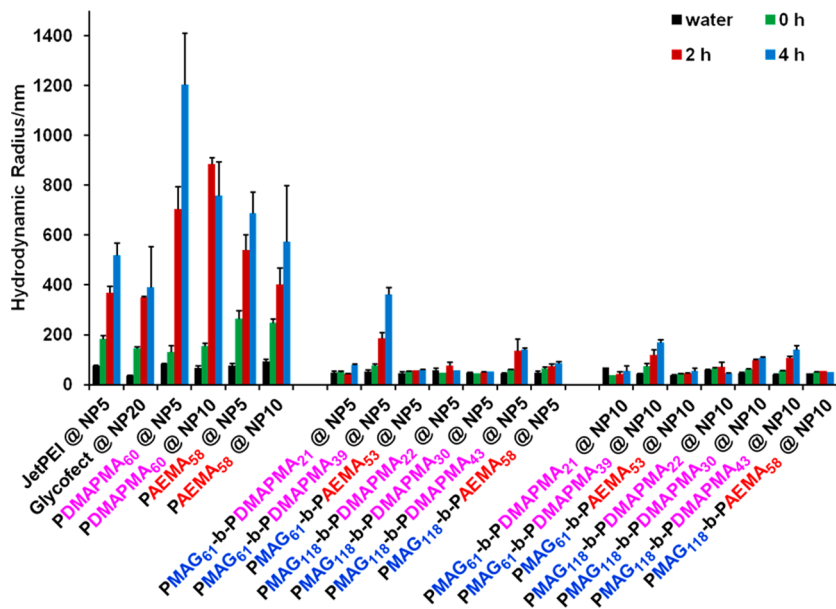


Figure 2. Hydrodynamic radius of polyplexes formed at *N/P* ratios of 5 and 10 at 0, 2, and 4 h after dilution with Opti-MEM. Error bars represent the standard deviation of analyzed data from three replicates.

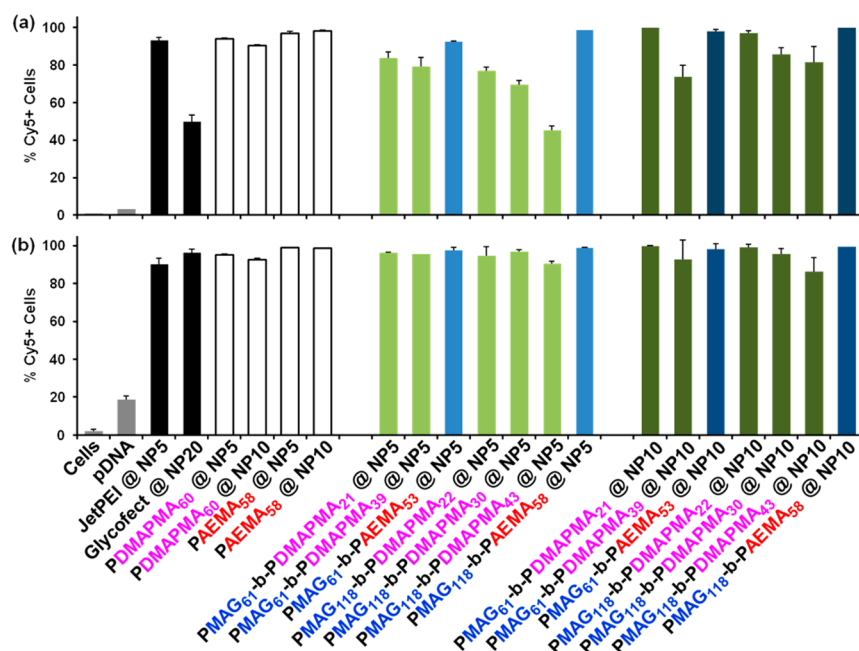


Figure 3. Percentage of Cy5 positive cells 4 h after transfection with polyplexes formed with Cy5-labeled pDNA at *N/P* ratios of 5 and 10 in (a) HeLa cells and (b) HepG2 cells. Error bars represent the standard deviation of analyzed data from three replicates.

around 50 nm to over 400 nm. Additionally, polyplexes formed from cationic homopolymers, PDMAPMA₆₀ and PAEMA₅₈, were found to aggregate in Opti-MEM, which was evident as the radius significantly increased from 50 nm to over 600 nm over a 4 h time period. On the contrary, glycopolymer polyplexes were relatively stable over the 4 h period, with the radius remaining around 50 nm in almost all cases; the size increase of PMAG₆₁-b-PDMPMA₃₉ polyplexes was observed at a *N/P* ratio of 5, probably due to the relatively weak association between pDNA and the tertiary amine block in this analog; interestingly, the aggregation was not as obvious at an *N/P* ratio of 10. These experimental results are consistent with previous published results, where the polyplexes composed of

block glycopolymers exhibited high colloidal stability in cell culture media.^{9,10,12} It is proposed that cationic block copolymers can condense pDNA with a core–shell structure.^{33,34} The stabilization effect is likely attributed to the shell of PMAG, which serves as a bulky hydrophilic coating, preventing the polyplexes from aggregating in Opti-MEM. The protective function of the PMAG block that coats the polyplexes becomes apparent when comparing the stability of glycopolymer polyplexes with that of polyplexes formed with the cationic homopolymers. As mentioned previously, the hydrodynamic radii of homopolymer-based polyplexes, without the protection of the glucose derived block, increased

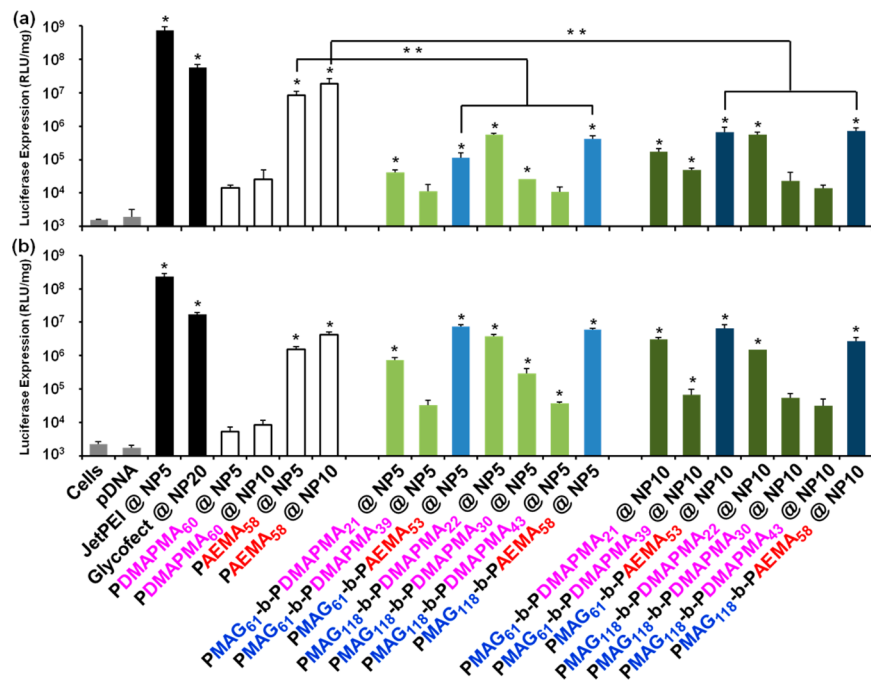


Figure 4. Luciferase gene expression (RLU/mg) 48 h after transfection with polyplexes formed at N/P ratios of 5 and 10 in (a) HeLa cells and (b) HepG2 cells. Error bars represent the standard deviation of analyzed data from three replicates. Measurements found to be statistically significant ($p < 0.05$) compared to cells only are marked with an asterisk. Double asterisks represent the statistically significant difference ($p < 0.05$) between data groups.

dramatically in Opti-MEM medium over the experimental period.

The in vitro internalization profiles of polyplexes formed from Cy5-labeled pDNA and the polymers were examined via flow cytometry 4 h after cells were exposed to the polyplex formulations. The percentage of Cy5 positive cells in live cells (Figure 3) and the mean fluorescence intensity (MFI, Supporting Information, Figure S10) were determined with a helium–neon laser to excite the Cy5 fluorophore at 633 nm wavelength. The cells only samples were utilized as negative controls to gate out the background fluorescence (<1%). Propidium iodide was also used as the reagent to stain and eliminate unhealthy cells from interfering with the analysis. With both HeLa cells and HepG2 cells, the cationic homopolymers, PDMAPMA₆₀ and PAEMA₅₈, were successfully internalized by about 95% of cells at N/P ratios of 5 and 10. With polyplexes formed by the PMAG-*b*-PAEMA series, over 92% of cells in both cell types were Cy5-pDNA positive. However, the polyplexes formulated with glycopolymers containing the DMAPMA blocks exhibited lower cellular internalization levels than that observed with the PMAG-*b*-PAEMA series at N/P ratios of 5 in HeLa cells. More specifically, the percentage of cells positive for Cy5-pDNA internalization percentage dropped when the DMAPMA block length increased. For example, the uptake level decreased from 77 to 45% when the PDMAPMA block length increased from 22 to 43 repeat units for the PMAG₁₁₈ series of polymers. This uptake percentage decrease was possibly due to the toxicity of the PMAG-*b*-PDMAPMA copolymers (vide infra); the cells that internalized the polyplexes formed with those block copolymers were found to be positive for propidium iodide staining. The internalization levels for polyplexes formed with the PMAG-*b*-PDMAPMA polymer series generally improved by increasing the N/P ratio from 5 to 10 in HeLa cells.

Interestingly, the polyplexes exhibited different cellular uptake profiles in HepG2 cells from that in HeLa cells. The internalization percentage of the glycopolymer polyplexes was generally comparable to that of the homopolymers in HepG2 cells. Moreover, for the PMAG-*b*-PDMAPMA polymer series, the Cy5-pDNA internalization percentages were all greater than 86% in HepG2 cells, while the uptake percentage varied from 45 to 84% at an N/P ratio of 5 in HeLa cells. Additionally, the MFI values per cell (fluorescent intensity \times uptake percentage) of the polyplexes tested were higher in HepG2 cells than in HeLa cells. This result indicates that more Cy5-pDNA, on average, was internalized by HepG2 cells than by HeLa cells (Supporting Information, Figure S10). The disparity of the mean intensity between the two cell types could be mainly caused by the inherent nature of these cell types. Although previous research has shown that hydrophilic stabilizing blocks, such as PEG, can hinder the cellular uptake of polyplexes by limiting the interaction between polyplexes and cellular membrane,⁴⁰ herein, we did not observe a notable difference in cellular internalization percentages between glycopolymers and the homopolymers, PAEMA₆₀ and PDMAPMA₅₈, in HepG2 cells. Also, polyplexes formed with the glycopolymers and homopolymers did not exhibit differences in internalization percentages in HeLa cells at an N/P of 10. These results suggested that the presence of the PMAG block coating did not hinder the ability of polyplexes to be internalized by cells.

To determine the capability of the polymers to express the delivered pDNA in vitro, both HeLa cells and HepG2 cells were treated with polyplexes composed of pDNA encoding firefly luciferase protein at N/P ratios of 5 and 10. A luciferase assay was carried out 48 h after transfection and the transfection efficiency was quantified by luminescence (relative light units) as a function of total protein expressed (Figure 4). In HeLa cells, glycopolymer polyplexes overall did not exhibit a

significant transfection efficiency compared with the commercial reagents, JetPEI (7.4×10^8 RLU/mg) and Glycofect (5.7×10^7 RLU/mg). Polyplexes formulated with the cationic homopolymer, PAEMA₅₈, exhibited significantly higher efficiency than polyplexes formulated with PDMAPMA₆₀. In addition, the transfection efficiency decreased when the PDMAPMA block length increased for the PMAG-*b*-PDMAPMA series. For example, at an N/P ratio of 5, the transgene expression level was 5.7×10^5 RLU/mg for PMAG₁₁₈-*b*-PDMAPMA₂₂ polyplexes, while the value dropped to 1.1×10^4 RLU/mg for PMAG₁₁₈-*b*-PDMAPMA₄₃ polyplexes. The low transfection efficiency of both the PDMAPMA₅₈ and PMAG-*b*-PDMAPMA polyplexes suggested that the PDMAPMA block is not very effective for pDNA delivery or promoting gene expression in HeLa cells. Aside from the toxicity of the PMAG-*b*-PDMAPMA copolymers playing a role in transfection, it was documented by Palermo et al. that polymers containing primary amines were more capable of binding and disrupting membranes compared to the polymers bearing tertiary amine structures (possibly related to endosomal escape).⁴¹ Palermo et al. examined the interaction between liposomes formed with the lipid 1-palmitoyl-2-oleoyl-sn-glycero-3-phosphocholine (POPC) and three polymethacrylate derivatives consisting of hydrophobic groups and primary, tertiary, or quaternary ammonium salt groups, and demonstrated that primary amine containing polymers achieved the highest dye leakage from liposome vesicles.⁴¹ Interestingly, PAEMA₆₀ homopolymers exhibited much higher transfection efficiency than the PMAG-*b*-PAEMA block copolymers in HeLa cells. At an N/P ratio of 5, the transfection efficiency for polyplexes formulated with PAEMA₅₈ was 8.3×10^6 RLU/mg in HeLa cells, while transfection efficiencies of polyplexes formulated with block glycopolymers PMAG₆₁-*b*-PAEMA₅₃ and PMAG₁₁₈-*b*-PAEMA₅₈ were 1.1×10^5 RLU/mg and 4.3×10^5 RLU/mg, respectively. At an N/P ratio of 10, the transfection efficiency increased for PAEMA₅₈ polyplexes. While a slight increase was noted in transfection efficiency for both PMAG₆₁-*b*-PAEMA₅₃ and PMAG₁₁₈-*b*-PAEMA₅₈ polyplexes at N/P = 10, it was still nearly 2 orders of magnitude lower than the PAEMA₅₈ homopolymer. Several previous reports have demonstrated that PEGylation could hinder the transfection efficiency of PEI due to shielding effects.^{42,43} Ahmed et al. reported the synthesis of a series of copolymers composed of AEMA and 2-methacryloxyethyl phosphorylcholine (MPC) for pDNA delivery, and the block copolymer PMPC₃₆-*b*-PAEMA₄₀ exhibited a lower transfection level than the cationic homopolymer analogue, PAEMA₅₈, by about 10 RLU/mg, according to a β -galactosidase assay.⁷ While the hydrophilic block could play some role in decreasing transfection efficiency/gene expression, herein, it is clear that the charge center type plays the largest role in promoting (or suppressing) effective transgene delivery.

In HepG2 cells, the transfection efficiency trend observed for the polyplexes formed with the PMAG-*b*-PDMAPMA series was similar to that in HeLa cells; as the PDMAPMA block length increased, the transfection efficiency decreased. More specifically, the transfection efficiency was 3.8×10^6 RLU/mg for PMAG₁₁₈-*b*-PDMAPMA₂₂ at an N/P ratio of 5, but the value dropped significantly to 3.7×10^4 RLU/mg for PMAG₁₁₈-*b*-PDMAPMA₄₃, in HepG2 cells. Additionally, the homopolymers, PDMAPMA₆₀, exhibited very low transgene expression levels (5.3×10^3 RLU/mg at an N/P ratio of 5) and had only slightly higher values at an N/P ratio of 10 (8.5×10^3 RLU/

mg) in HepG2 cells. These results further suggest that the PDMAPMA blocks did not possess the ability for pDNA delivery in this study. In addition, it was found that the homopolymer PAEMA₅₈ did not have the highest transfection efficiency in HepG2 cells. Interestingly, the PMAG-*b*-PAEMA series yielded the highest transfection efficiency, indicating that this cell type may offer a preference for promoting higher transgene expression for the vehicles containing the MAG blocks.

The direct comparison of the transfection efficiency between cell lines revealed that polyplexes formulated with the block glycopolymers exhibited higher transfection levels in HepG2 cells than in HeLa cells (Supporting Information, Figure S11). For example, for the copolymer PMAG₆₁-*b*-PDMAPMA₂₁, the transfection efficiency at an N/P ratio of 5 was 7.4×10^5 RLU/mg in HepG2 cells, but 4.2×10^4 RLU/mg in HeLa cells. As we established in the cellular uptake experiments, the intensity of Cy5-pDNA was higher in HepG2 cells than in HeLa cells on average (Supporting Information Figure S10). Therefore, the higher observed transfection efficiency in HepG2 cells could be, in part, due to the higher cellular internalization. Furthermore, the homopolymers, PAEMA₅₈, and the block copolymer PMAG-*b*-PAEMA series exhibited comparable transfection efficiency in HepG2 cells. At an N/P ratio of 5, the transgene expression level in HepG2 cells for PAEMA₅₈ was found to be 1.6×10^6 RLU/mg, and the expression levels for PMAG₆₁-*b*-PAEMA₅₃ and PMAG₁₁₈-*b*-PAEMA₅₈ were higher (7.6×10^6 RLU/mg and 5.9×10^6 RLU/mg, respectively). At the higher N/P ratio of 10, the level of gene expression was similar. Interestingly, as previously mentioned, this trend was not found with HeLa cells; the homopolymer, PAEMA₅₈, exhibited much higher transfection (2 orders of magnitude) than the block copolymers. These results suggested that the PMAG block may have beneficial interactions with HepG2 cells than with HeLa cells, resulting in increased *in vitro* pDNA delivery. These experimental results reveal that the PDMAPMA block was not an ideal charge center structure to promote high transfection efficiency in either cell type. Furthermore, the PMAG block serves as both a hydrophilic coating to prevent colloidal aggregation and appears to also impact the pDNA delivery efficiency in a cell type dependent manner, possibly due to the varied interaction between glycopolymer-coated polyplexes and different cellular membranes.

There are approximately 150000 to 250000 asialoglycoprotein (ASGP) receptors per cell present on the hepatocellular membrane.⁴⁴ The ASGP receptors were discovered to specifically recognize terminal β -linked galactose or *N*-acetylglucosamine (GlcNAc) residues, and to mediate endocytosis.^{44,45} Due to the function of ASGP receptors, they have been heavily exploited for targeted nucleic acid delivery to liver hepatocytes.^{44,46,47} However, ASGP receptors are not present on HeLa cell membranes.⁴⁸ The transfection efficiency comparison between the PAEMA₅₈ homopolymer and the PMAG-*b*-PAEMA glycopolymers revealed that the PMAG block impacted efficiency between the two cell types. The presence of the PMAG block reduced the transfection efficiency in HeLa cells, yet appeared to be beneficial for pDNA delivery in HepG2 cells. As the ASGP receptors are a unique feature of HepG2 cells, it is hypothesized that the PMAG block could interact with ASGP receptors on cellular membrane, and such interaction could facilitate the pDNA delivery for block glycopolymers in HepG2 cells. To test this hypothesis, both HeLa cells and HepG2 cells were treated with

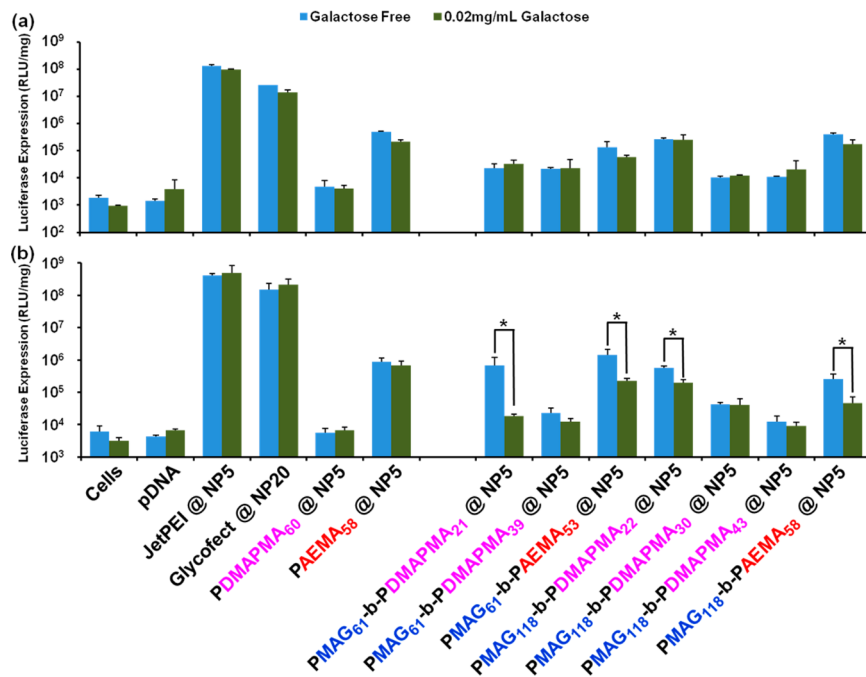


Figure 5. Luciferase gene expression (RLU/mg) 48 h after transfection with polyplexes formed at N/P ratios of 5 and 10 in (a) HeLa cells and (b) HepG2 cells, treated with and without galactose containing DMEM. Error bars represent the standard deviation of analyzed data from three replicates. Measurements found to be statistically different ($p < 0.05$) are marked with asterisk.

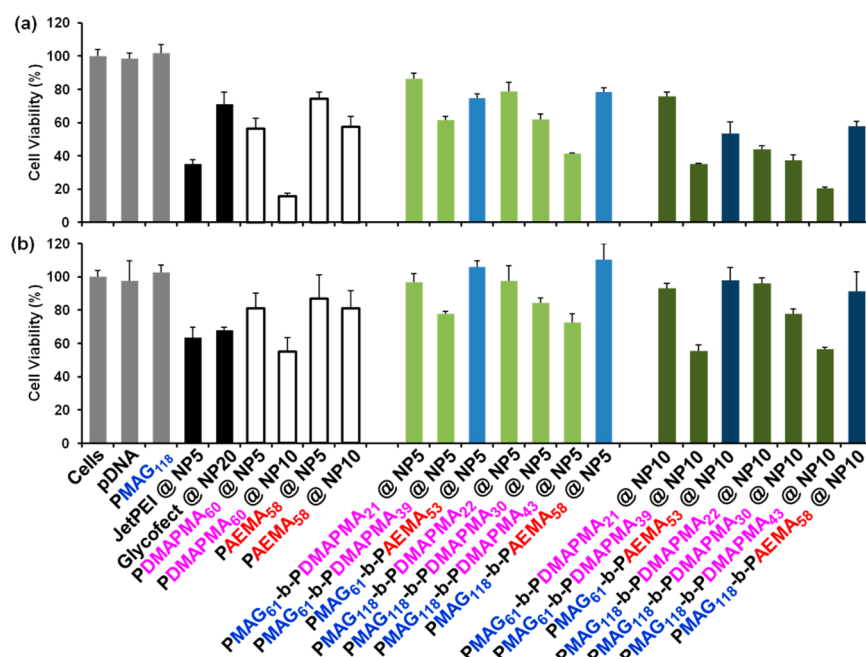


Figure 6. Cell viability 48 h after transfection with glycopolymer/pDNA polyplexes in (a) HeLa cells and (b) HepG2 cells, as determined by an MTT assay. Error bars represent the standard deviation of the analyzed data from three replicates.

a solution of 0.02 mg/mL D-(+)-galactose in DMEM for 20 min prior to the exposure to the polyplexes. Owing to the high affinity that the ASGP receptor has for galactose, the carbohydrate binding site of the receptor would be occupied by galactose, it would hence decrease interactions with the glycopolymers after the treatment. DMEM without galactose was also used to treat cells for the same period of time as a control. Figure 5 displays the transfection efficiency of both the control group and the group exposed to galactose (inhibition treatment). For several diblock copolymers (PMAG₆₁-b-

PDMAPMA₂₁, PMAG₆₁-b-PAEMA₅₃, PMAG₁₁₈-b-PDMAPMA₂₂, PMAG₁₁₈-b-PAEMA₅₈) the treatment of HepG2 cells with DMEM containing galactose resulted in lower transgene expression. Such a difference in the transfection conditions was not observed in HeLa cells for polyplexes formulated with the diblock glycopolymers. Moreover, galactose containing DMEM treatment did not impact, with either cell line, the transfection efficiency of polyplexes formed with the cationic homopolymers nor the positive controls (commercial reagents). These results indicate that the presence of galactose molecules

inhibited pDNA delivery in HepG2 cells for the block glycopolymer polyplexes. These data reveal that between the two cell types, the polyplexes formulated with the glycopolymers may have an increase in interactions with HepG2 cell membranes. More importantly, such interaction facilitated transgene expression, as the inhibition of this receptor with galactose decreased gene expression with the glycopolymer-based polyplexes in HepG2 cells. These results suggest that the polymerized glucose moieties within the PMAG block facilitates an interaction (potentially with the ASGP receptors) on the HepG2 cell membrane. This premise is further supported by the data showing that the transfection efficiency of the cationic homopolymers, PDMAPMA₆₀ and PAEMA₅₈, was not altered by the addition of galactose. Additionally, MTT assays revealed that the galactose containing DMEM treatment did not alter the viability of cells exposed to polyplexes throughout the course of the transfection experiment (Supporting Information, Figure S12). Thus, cell viability was not a factor in the decrease in gene expression for cells treated with galactose, which further supports our hypothesis that the poly(MAG) block aids internalization.

The cytotoxicity of the polyplexes was determined through MTT assays with both cell lines (Figure 6). Polyplexes generally exhibited higher cytotoxicity in HeLa cells than in HepG2 cells. In HepG2 cells, most of the polyplexes exhibited over 80% cell survival 48 h after transfection. It was found that the cytotoxicity of polyplexes increased as both the PDMAPMA block length and the N/P ratio increased in both cell lines. Because the PMAG block alone (no charge block) did not exhibit cytotoxicity according to MTT assays, it can be deduced that the toxic effects stem from the polyamine block. Previous work has demonstrated that the cytotoxicity of polyplexes could be partially caused by nuclear membrane permeation.⁴⁹ However, a more in-depth study is needed to determine the major mechanism of toxicity for this series of polymers, in particular, the distinct rationale for the higher toxicity of the PDMAPMA block copolymers.

CONCLUSION

This study reported the synthesis of a series of diblock glycopolymers for pDNA delivery. The glycopolymers exhibited the ability to bind pDNA at low N/P ratios and form polyplexes. The PMAG block was found to improve the colloidal stability of polyplexes in physiological salt solutions when compared to systems not stabilized by a hydrophilic block. The internalization profile, transgene expression efficiency and cytotoxicity of the polyplexes exhibited a large dependency upon the architecture (amine type and block length) during in vitro transfection experiments in both HeLa and HepG2 cells. Generally, polyplexes formed with glycopolymers with a PAEMA block showed higher transfection efficiency than glycopolymers with PDMAPMA block. Moreover, glycopolymers with a longer PDMAPMA block length appeared to be less efficient gene delivery vehicles with higher cytotoxicity. The length of the PMAG block did not show a significant impact on the pDNA delivery in the current study. Interestingly, glycopolymer polyplexes exhibited much higher transfection efficiency in HepG2 cells than in HeLa cells. This was attributed to the ability of HepG2 cells to both internalize more polyplexes and promote higher gene expression, in comparison with the same systems in HeLa cells. Comparing the transfection efficiency between PAEMA₅₈ lacking the sugar block and PMAG-*b*-PAEMA systems in the two cell types, it

was revealed that the PMAG block could have interactions with specific receptors on hepatocellular membranes. The interaction between the exposed PMAG block on polyplexes and HepG2 cells could contribute to the increased transfection efficiency in HepG2 cells. The presence of galactose molecules in the media inhibited the transgene expression for some of the glycopolymers in HepG2 cells, potentially indicating that the ASGP receptor could play a role in this enhanced delivery profile. Further studies are needed to explore the intracellular pathways associated with these glycopolymer pDNA delivery systems and the potential mechanism of cytotoxicity associated with the PDMAPMA block.

ASSOCIATED CONTENT

S Supporting Information

Additional SEC chromatograms, ¹H NMR spectra, gel electrophoresis images, and transgene expression efficiency comparison between cell lines are included. This material is available free of charge via the Internet at <http://pubs.acs.org>.

AUTHOR INFORMATION

Corresponding Author

*E-mail: treineke@umn.edu.

Notes

The authors declare no competing financial interest.

ACKNOWLEDGMENTS

The authors would like to thank Dr. Nilesh P. Ingle, Department of Chemistry, University of Minnesota, and Dr. B. Kevin Anderson, Department of Chemistry, Oakwood University, for consistent help on cell experiments. We also would like to acknowledge Timothy R. Pearce, Department of Chemical Engineering and Material Science, University of Minnesota, and Dr. Bob Hafner, Characterization Facility, University of Minnesota, for the technical assistance on cryoTEM imaging. The project is funded by National Institutes of Health Director's New Innovator Award Program (DP2OD006669-02). Parts of this work were carried out in the Institute of Technology Characterization Facility, University of Minnesota, a member of the NSF-funded Materials Research Facilities Network.

REFERENCES

- (1) Kay, M. A. *Nat. Rev. Genet.* **2011**, *12*, 316–328.
- (2) Mintzer, M. A.; Simanek, E. E. *Chem. Rev.* **2009**, *109*, 259–302.
- (3) Davis, M. E.; Zuckerman, J. E.; Choi, C. H. J.; Seligson, D.; Tolcher, A.; Alabi, C. A.; Yen, Y.; Heidel, J. D.; Ribas, A. *Nature* **2010**, *464*, 1067–1070.
- (4) Wang, T.; Upponi, J. R.; Torchilin, V. P. *Int. J. Pharm.* **2012**, *427*, 3–20.
- (5) Oba, M.; Miyata, K.; Osada, K.; Christie, R. J.; Sanjoh, M.; Li, W.; Fukushima, S.; Ishii, T.; Kano, M. R.; Nishiyama, N.; Koyama, H.; Kataoka, K. *Biomaterials* **2011**, *32*, 652–663.
- (6) Xu, Y.; Takai, M.; Ishihara, K. *Biomaterials* **2009**, *30*, 4930–4938.
- (7) Ahmed, M.; Bhuchar, N.; Ishihara, K.; Narain, R. *Bioconjugate Chem.* **2011**, *22*, 1228–1238.
- (8) Hemp, S. T.; Smith, A. E.; Bryson, J. M.; Allen, M. H.; Long, T. E. *Biomacromolecules* **2012**, *13*, 2439–2445.
- (9) Smith, A. E.; Sizovs, A.; Grandineti, G.; Xue, L.; Reineke, T. M. *Biomacromolecules* **2011**, *12*, 3015–3022.
- (10) Li, H.; Cortez, M. A.; Phillips, H. R.; Wu, Y.; Reineke, T. M. *ACS Macro Lett.* **2013**, *2*, 230–235.
- (11) Buckwalter, D. J.; Sizovs, A.; Ingle, N. P.; Reineke, T. M. *ACS Macro Lett.* **2012**, *1*, 609–613.

- (12) Ahmed, M.; Jawanda, M.; Ishihara, K.; Narain, R. *Biomaterials* **2012**, *33*, 7858–7870.
- (13) Ahmed, M.; Narain, R. *Biomaterials* **2011**, *32*, 5279–5290.
- (14) Wang, Y.; Hong, C.-Y.; Pan, C.-Y. *Biomacromolecules* **2013**, *14*, 1444–1451.
- (15) Ahmed, M.; Narain, R. *Biomaterials* **2012**, *33*, 3990–4001.
- (16) Knop, K.; Hoogenboom, R.; Fischer, D.; Schubert, U. S. *Angew. Chem., Int. Ed.* **2010**, *49*, 6288–6308.
- (17) Barz, M.; Luxenhofer, R.; Zentel, R.; Vicent, M. J. *Polym. Chem.* **2011**, *2*, 1900–1918.
- (18) Ting, S. R. S.; Chen, G.; Stenzel, M. H. *Polym. Chem.* **2010**, *1*, 1392–1412.
- (19) Orietta, L.; Alexandra, M.-B.; Vanesa, B.; Manuel, S.-C.; Marta, F.-G. *J. Polym. Sci., Part A: Polym. Chem.* **2011**, *49*, 2627–2635.
- (20) Alexandra, M.-B.; Orietta, L.; Vanesa, B.; Manuel, S.-C.; Marta, F.-G. *J. Polym. Sci., Part A: Polym. Chem.* **2013**, *51*, 1337–1347.
- (21) Song, E.-H.; Manganiello, M.; Chow, Y.-H.; Ghosn, B.; Convertine, A.; Stayton, P.; Schnapp, L.; Ratner, D. *Biomaterials* **2012**, *33*, 6889–6897.
- (22) Smith, D.; Holley, A. C.; McCormick, C. L. *Polym. Chem.* **2011**, *2*, 1428–1441.
- (23) Hawker, C. J.; Bosman, A. W.; Harth, E. *Chem. Rev.* **2001**, *101*, 3661–3688.
- (24) Matyjaszewski, K. *Macromolecules* **2012**, *45*, 4015–4039.
- (25) Moad, G.; Rizzardo, E.; Thang, S. H. *Aust. J. Chem.* **2005**, *58*, 379–410.
- (26) Ahmed, M.; Narain, R. *Prog. Polym. Sci.* **2013**, *38*, 767–790.
- (27) Mitsukami, Y.; Donovan, M. S.; Lowe, A. B.; McCormick, C. L. *Macromolecules* **2001**, *34*, 2248–2256.
- (28) Convertine, A. J.; Lokitz, B. S.; Vasileva, Y.; Myrick, L. J.; Scales, C. W.; Lowe, A. B.; McCormick, C. L. *Macromolecules* **2006**, *39*, 1724–1730.
- (29) Xu, X.; Smith, A. E.; Kirkland, S. E.; McCormick, C. L. *Macromolecules* **2008**, *41*, 8429–8435.
- (30) York, A. W.; Huang, F.; McCormick, C. L. *Polym. Prepr. (Am. Chem. Soc., Div. Polym. Chem.)* **2008**, *49*, 1099–1100.
- (31) Kirkland-York, S.; Zhang, Y.; Smith, A. E.; York, A. W.; Huang, F.; McCormick, C. L. *Biomacromolecules* **2010**, *11*, 1052–1059.
- (32) York, A. W.; Huang, F.; McCormick, C. L. *Biomacromolecules* **2010**, *11*, 505–514.
- (33) Ziebarth, J.; Wang, Y. *J. Phys. Chem. B* **2010**, *114*, 6225–6232.
- (34) Nakai, K.; Nishiuchi, M.; Inoue, M.; Ishihara, K.; Sanada, Y.; Sakurai, K.; Yusa, S.-i. *Langmuir* **2013**, *29*, 9651–9661.
- (35) Pearson, S.; Allen, N.; Stenzel, M. H. *J. Polym. Sci., Part A: Polym. Chem.* **2009**, *47*, 1706–1723.
- (36) Nie, C.; Liu, C.; Chen, G.; Dai, J.; Li, H.; Shuai, X. *J. Biomater. Appl.* **2011**, *26*, 255–275.
- (37) Won, Y.-Y.; Sharma, R.; Konieczny, S. F. *J. Controlled Release* **2009**, *139*, 88–93.
- (38) Levine, R. M.; Pearce, T. R.; Adil, M.; Kokkoli, E. *Langmuir* **2013**, *29*, 9208–9215.
- (39) Liu, Y.; Reineke, T. M. *J. Am. Chem. Soc.* **2005**, *127*, 3004–3015.
- (40) Gomes-da-Silva, L. C.; Fonseca, N. A.; Moura, V.; Pedroso de Lima, M. C.; Simões, S.; Moreira, J. N. *Acc. Chem. Res.* **2012**, *45*, 1163–1171.
- (41) Palermo, E. F.; Lee, D.-K.; Ramamoorthy, A.; Kuroda, K. *J. Phys. Chem. B* **2011**, *115*, 366–375.
- (42) Luo, X.; Feng, M.; Pan, S.; Wen, Y.; Zhang, W.; Wu, C. *J. Mater. Sci.: Mater. Med.* **2012**, *23*, 1685–1695.
- (43) Sung, S.-J.; Min, S. H.; Cho, K. Y.; Lee, S.; Min, Y.-J.; Yeom, Y. I.; Park, J.-K. *Biol. Pharm. Bull.* **2003**, *26*, 492–500.
- (44) Wu, G. Y.; Wu, C. H. *Adv. Drug Delivery Rev.* **1998**, *29*, 243–248.
- (45) Rigopoulou, E. I.; Roggenbuck, D.; Smyk, D. S.; Liaskos, C.; Mytilinaiou, M. G.; Feist, E.; Conrad, K.; Bogdanos, D. P. *Autoimmun. Rev.* **2012**, *12*, 260–269.
- (46) Pathak, A.; Vyasa, S. P.; Gupta, K. C. *Int. J. Nanomed.* **2008**, *3*, 31–49.
- (47) Fukuma, T.; Wu, G. Y.; Wu, C. H. *Gene Ther. Regul.* **2000**, *1*, 79–93.
- (48) Pun, S. H.; Davis, M. E. *Bioconjugate Chem.* **2002**, *13*, 630–639.
- (49) Grandinetti, G.; Smith, A. E.; Reineke, T. M. *Mol. Pharmaceutics* **2011**, *9*, 523–538.